Dalton Transactions

Accepted Manuscript

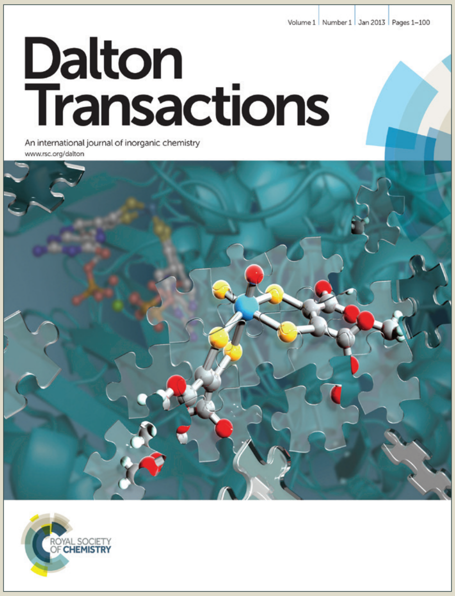

Ultrafast photophysical processes for Fe(III)-carboxylates

Ivan P. Pozdnyakov[a,b], Alexey A. Melnikov[c], Nikolai Tkachenko[d], Sergey V. Chekalin[c], Helge Lemmetyinen[d], Victor F. Plyusnin[a,b]

[a]*Institute of Chemical Kinetics and Combustion, Siberian Branch of Russian Academy of Sciences, Institutskaya 3, 630090 Novosibirsk, Russian Federation*

[b]*Novosibirsk State University, Pirogova 2, 630090 Novosibirsk, Russian Federation*

[c]*Institute of Spectroscopy, Russian Academy of Sciences, Physicheskaya 5, 142190 Troitsk, Moscow, Russian Federation*

[d]*Department of Chemistry and Bioengineering, Tampere University of Technology, 33101, Korkeakoulunkatu 8, Tampere, Finland*

Abstract

Photochemical reactions with participation of iron (III) carboxylates are important for environmental photochemistry and have a great potential of application in water purification (Advanced Oxidation Processes, photo-Fenton and Fenton-like processes). In spite of this information about excited states and primary intermediates in photochemistry of Fe(III) complexes with carboxylic acids is scarce. This mini-review presents and discusses the results of several recent publications in a field of ultrafast spectroscopy of natural Fe(III) carboxylates.

Keywords: photochemistry, iron complexes, carboxylates, radical complexes, ultrafast processes

Introduction

Photochemical reactions of Fe(III) - (poly)carboxylate complexes influence on many iron-dependent biogeochemical processes and are responsible for photochemical production of CO, CO_2 and for oxygen consumption in natural waters.[1-4] It is assumed, that photolysis of Fe(III)-(poly)carboxylate complexes is one of the main sources of reactive oxygen species (ROS - $^{\bullet}OH$, $HO_2^{\bullet}$, H_2O_2), which formation is catalyzed by Fe(II) and Fe(III) ions in Fenton-like reactions.[4-7] ROS influence on the chemical composition and the red-ox capacity of natural water systems, in particular providing oxidation of sulfur- and nitrogen-containing compounds in the atmosphere.[8,9]

Historically it was typically believed that the primary process in the photochemistry of Fe(III) complexes with aliphatic (poly)carboxylic acids (further Fe(III)-ALCA) is an inner-sphere electron transfer with the formation of Fe(II) and an escape of an organic radical to the solution bulk (reaction 1)[6,7,10] followed by its fast decarboxylation (reaction 2) [11,12]:

$$[\text{Fe–OOC–R}]^{2+} + h\nu \longrightarrow \text{Fe}^{2+} + \text{R–COO}^{\bullet} \qquad (1)$$

$$\mathrm{R{-}COO^{\bullet}} \longrightarrow \mathrm{R^{\bullet}} + \mathrm{CO_2} \qquad (k \sim 10^{9}\ \mathrm{s^{-1}}) \tag{2}$$

The secondary radical formed as the result of decarboxylation could react with the different components of the reaction system (e.g., Fe(III) complexes or molecular oxygen). ROS are formed consequently which provide the mineralization of organic compounds in natural waters.[6,7,10]

The reaction mechanism (1-2) was put forward based on results of stationary experiments. Recently nanosecond laser flash photolysis (LFP) technique was used to clarify the mechanism of photolysis of Fe(III)-ALCA complexes.[13–16] The main intermediate in photochemistry of Fe(III) complexes with several natural organic acids (lactic, $[\mathrm{Fe(Lact)}]^{+}$, tartaric, ($[\mathrm{Fe(Tart)}]^{+}$; pyruvic, $[\mathrm{Fe(Pyr)}]^{2+}$; oxalic $[\mathrm{Fe(Ox)_3}]^{3-}$ and glyoxalic $[\mathrm{Fe(AG)}]^{2+}$) was found to be corresponding long-lived radical complex rather than short-lived organic radical (the yield of organic radicals in primary process is not exceed 7% for all studied complexes)[15]:

$$[\mathrm{Fe{-}OOC{-}R}]^{2+} + h\nu \longrightarrow [\mathrm{Fe^{II}}\ldots{}^{\bullet}\mathrm{OOC{-}R}]^{2+} \tag{3a}$$

Fe(II)-radical complexes exhibits a weak absorption band in visible region (maximum at 620-670 nm) and monoexponential decay in millisecond time scale (1 – 5 ms) due to dissociation and reaction with dissolved oxygen ($k = (1\text{-}3)\times10^{6}\ \mathrm{M^{-1}s^{-1}}$).[13–16] The formation of long-lived radical complexes is a common case in the photochemistry of transition metals, which was shown for the number of coordination compounds (including carboxylate complexes of Fe(III) and Co(III)).[17-19] Long lifetime of the Fe(II) radical complex could be explained by the essential elongation of Fe-O bonds (difference between Fe(II)-O and Fe(III)-O bonds is about ≈0.2 A)[20,21] leading to the large structural changes in the Fe(II)-radical complex. This structural difference may result in a potential barrier preventing back electron transfer. Another reason of stability of the radical complexes could be fast $\mathrm{CO_2}$ detachment after inner-sphere electron transfer with formation of $[\mathrm{Fe(II)}\ldots\mathrm{R^{\bullet}}]$ radical complex:

$$[\mathrm{Fe{-}OOC{-}R}]^{2+} + h\nu \longrightarrow [\mathrm{Fe^{II}}\ldots\mathrm{R^{\bullet}}]^{2+} + \mathrm{CO_2} \tag{3b}$$

Current LFP data don't allow to distinguish between mechanisms (3a) and (3b) and additional experiments with involvement of ESR technique and quantum-chemistry calculations are needed to clarify the situation.

It is known that quantum yield of Fe(II) formed by photolysis of Fe(III)-ALCA complexes depends rather weakly on excitation wavelength (λ_{ex}) and is equal 1.25 for Fe(III)-oxalate (λ_{ex} = 260 - 365 nm[22]), ≈ 0.28 for Fe(III)-citrate (λ_{ex} = 366 [23] and 436 [7] nm) ≈ 0.5 for Fe(III)-tartrate (λ_{ex} = 313 - 366 nm[15, 23-25]) and ≈ 0.4 for Fe(III)–lactate (313 – 366[15, 25] nm) complexes, accordingly. This fact indicates that the formation of the Fe(II) radical complex is taking place from the certain thermalized excited state of corresponding Fe(III)-ALCA complex.

Ultrafast processes for Fe(III)-ALCA complexes

Unfortunately, information about excited states of Fe(III) complexes with aliphatic acids is scarce. Few publications concerning ultrafast spectroscopy of Fe(III)-ALCA complexes could be found in literature.[16,21,26] It is worth to note that the investigation of femtochemistry of these complexes is a challenge for experimentalists due to rather low absorption coefficients of initial compounds and transient species.

In works[16,26] pump-probe spectroscopy (λ_{ex} = 320 and 400 nm) was used to study ultrafast processes for $[Fe(Lact)]^+$, $[Fe(Tart)]^+$ and [Fe(Cit)] in femto- picosecond time domain. Both excitation wavelengths (400 and 320 nm) fall to the same broad LMCT band of the complexes[27] from right and left side of the maximum of the absorption band, accordingly (Fig. 1).

The excitation of the Fe(III)-ALCA complexes with a femtosecond pulse (λ_{ex} = 400 nm) leads to the formation of transient absorption which is almost completely decayed in 30 ps. Kinetic curves at several selected wavelengths for $[Fe(Tart)]^+$ and [Fe(Cit)] complexes are presented in Figure 2a,b. The global analysis of the time profile in the wavelength range 440 – 760 nm by iterative reconvolution shows that the use of a two-exponential function (4) with the instrument response function gives a good fitting with the time constants collected at Table 1.

$$\Delta A(\lambda, t) = A_1(\lambda)e^{-\frac{t}{\tau_1}} + A_2(\lambda)e^{-\frac{t}{\tau_2}} + A_3(\lambda) \qquad (4)$$

Similar biphasic dynamics was also observed for the Fe(III)-ALCA complexes upon LMCT band excitation at 320 nm (Figure 3a,b).

The first process with observed time constant τ_1 was assigned to combination of an ultrafast vibrational cooling and solvent relaxation of Frank-Condon excited state to the thermalized one. This situation is typical for relaxation of Frank-Condon excited states of transition metal complexes in polar solvents exhibiting inertial solvation time about 100 fs.[28] One can expect that relaxation of the Frank-Condon excited state leads to some narrowing of absorption band due to vibrational relaxation[29] as indeed was observed experimentally (Figure 3a, Figure 4a,b).

The thermalized excited state decays with time constant τ_2 at a longer timescale leading to formation of the constant bleaching in UV part of spectrum and practically zero signal in the visible (Figure 3b; Figure 2b). This is good coinciding with the data obtained by nanosecond laser flash photolysis technique.[15] It is worth to note that characteristic absorption bands of $[Fe^{II}...{}^{\bullet}OOC–R]^{2+}$ complexes (λ_{max} = 620-650 nm, recorded by nanosecond laser flash photolysis[13-15] were not observed in femtosecond experiments with $[Fe(Tart)]^+$ and [Fe(Cit)] complexes. This is due to the extremely low absorption coefficients of the radical complexes (ε^{620} = 18 $M^{-1}cm^{-1}$ for $[Fe(tart)]^+$).[15] For $[Fe(Lact)]^+$ complex very weak long-lived component ($A_3(\lambda)$) was observed which spectrum is in good agreement with spectrum of $[\mathrm{Fe^{II}}\ldots\mathrm{–O—CH(Me)—COO^{\bullet}}]^{+}$ radical complex ($\varepsilon^{670} = 60$ M^{-1}cm^{-1}).[16] So authors[16,26] conclude that the thermalized excited state decays with time constant τ_2 by two processes – internal conversion to the ground state and formation of the long-lived Fe(II) radical complex in reaction (3a) or (3b). The competition of these processes determines the quantum yield of photolysis of Fe(III)-ALCA complexes.

In works[21,30] the photochemistry of $\mathrm{Fe^{III}(C_2O_4)_3^{3-}}$ was investigated by combination of time-resolved EXAFS spectroscopy, flash photolysis with different time resolution (from femto- to milliseconds), radical scavenging technique and theoretical calculations. Ultrafast formation (< 2-3 ps) of an absorption band with a maximum near 430 nm (Table 1) was observed upon excitation at 400 nm which was assigned to excited state of the $\mathrm{Fe^{III}(C_2O_4)_3^{3-}}$. At 4 and 9 ps after excitation the length of Fe-O bond was found to decrease from 2.02 (the ground state of $\mathrm{Fe^{III}(C_2O_4)_3^{3-}}$) to 1.93 and 1.87 Å accordingly. Taking into account, that experimental values of Fe(II)-O bonds are always higher than Fe(III)-O,[20,21] primary photoprocess was proposed to be Fe-O bond cleavage in the excited state with formation of five-coordinated $\mathrm{[(C_2O_3)O\text{-}Fe^{III}(C_2O_4)_2]^{3-}}$ intermediate. This process is accompanied by the C-C bond cleavage of the ligand leading to formation of tetrahedral-like four-coordinated $\mathrm{Fe^{III}(C_2O_4)_2^{-}}$ complex and $\mathrm{CO_2^{\bullet-}}$ radical:

$$^{*}[\mathrm{Fe^{III}(C_2O_4)_3^{3-}}] \longrightarrow \mathrm{[(C_2O_3)O\text{-}Fe^{III}(C_2O_4)_2]^{3-}} \longrightarrow \mathrm{Fe^{III}(C_2O_4)_2^{-}} + 2\mathrm{CO_2^{\bullet-}} \qquad (5)$$

$$^{*}[\mathrm{Fe^{III}(C_2O_4)_3^{3-}}] \longrightarrow \mathrm{Fe^{III}(C_2O_4)_2^{-}} + 2\mathrm{CO_2^{\bullet-}} \qquad (6)$$

Authors[21,30] couldn't distinguish between Reactions (5) and (6) due to insufficient time resolution of EXAFS method. For both $\mathrm{[(C_2O_3)O\text{-}Fe^{III}(C_2O_4)_2]^{3-}}$ and $\mathrm{Fe^{III}(C_2O_4)_2^{-}}$ theoretical calculations predict Fe-O bond length about 1.9 Å. Existence of reactions (5) and (6) was also supported by more than 50% decrease of Fe(II) quantum yield by the addition of radical scavenger (thymine) in ferrioxalate solution.

The interpretation[21,30] was contradictory to the mechanism based on formation of the radical complex $\mathrm{[(C_2O_4)_2Fe^{II}(C_2O_4^{\bullet})]^{3-}}$ as a primary photoproduct and to the very low quantum yield of organic radicals observed in nanosecond flash photolysis of $\mathrm{Fe^{III}(C_2O_4)_3^{3-}}$.[13] Alternative interpretation of EXAFS data[21],[30] was done in work[31] in which variation of Fe-O bond length during the first 10 ps after excitation was linked to population and thermal relaxation of the long-lived thermally equilibrated secondary excited state (THEXI state)[28] of $\mathrm{Fe^{III}(C_2O_4)_3^{3-}}$. Decay of the THEXI state leads to formation of the $\mathrm{[(C_2O_4)_2Fe^{II}(C_2O_4^{\bullet})]^{3-}}$ radical complex observed by nanosecond flash photolysis.[13] Following discussion[31] of the results of two groups[13,21] leads to conclusion that both interpretations need to be supported by additional femtochemistry experiments and quantum-chemistry calculation. Therefore, the primary stage of the mechanism of photolysis of Fe(III)-ALCA complexes is still open for discussion.

Ultrafast processes for Fe(III) complexes with aromatic carboxylates

In contrast to Fe(III)-ALCA complexes which demonstrate good quantum yields of Fe(II) production upon LMCT band excitation[7,15,22-25] Fe(III) complexes with derivatives of salicylic acid (aromatic carboxylates, SADs) demonstrate excellent photochemical stability.[32,33] SADs refers to aromatic carboxylic acids and can serve as model compounds for investigating photochemical properties of natural humic and fulvic acids and their complexes with Fe(III) ions.

In works[32,33] pump-probe spectroscopy (λ_{ex} = 420 and 530 nm) was used to study the reasons of photostability of Fe(III) complexes with 5-sulfosalicylic acid (SSA) with 1, 2 and 3 SSA molecules in the coordination sphere. All $Fe(SSA)_n$ (n = 1-3) complexes exhibit LMCT bands[34] in visible region (Figure 5a) which maximum shifts to UV with increasing of ligand number in coordination sphere of Fe(III). It was known that steady-state irradiation in region of LMCT bands does not cause any photodegradation of aqueous solutions of $Fe(SSA)_n$ complexes.[32]

It was observed that excitation of the $Fe(SSA)_n$ complexes with a femtosecond pulse leads to biphasic dynamics of evolution of transient absorption which is almost completely decayed in 5 ps (Figure 5b). Initial intermediate with the absorption spectrum (Figure 6a, curve 1) exhibiting great red shift (~150 nm) comparing with ground state absorption spectrum (Figure 6a, curve 3) was assigned to Frank-Condon electronic excited state. This state undergoes an ultrafast (100 – 300 fs, Table 2) back electron transfer (ET) to the vibrationally hot electronic ground state. The population of vibrationally hot electronic ground state of $Fe(SSA)_n$ leads to blue shift of transient absorption spectra (Figure 6a, curve 2) of 60-80 nm comparing with absorption spectrum of Frank-Condon electronic excited state. It is worth to note that the absorption maximum of the hot ground state of $Fe(SSA)_n$ is close to the maximum of thermilized ground state, but the width of the former is much higher due to redistribution of vibrational energy on several vibrational modes. The hot ground state of $Fe(SSA)_n$ is thermalized in picosecond time domain (1 – 5 ps, Table 2) by vibrational cooling.[35,36] Generalized potential energy surface diagram for excited-state evolution of $Fe(SSA)_n$ complexes is shown in Figure 6b.

Conclusions

In the case of $Fe(SSA)_n$ complexes the ultrafast back ET to the ground state prevents the formation of $[Fe(II)(SSA)_{n-1}\ldots SSA^{2-\bullet}]$ radical pair and escape of $SSA^{2-\bullet}$ radical from coordination sphere of the complexes. This is the reason of observed photochemical stability of the complexes under irradiation in the LMCT band. Most probably that different photochemical behavior of aliphatic and aromatic carboxylates is related to different nature of organic radical formed by electron transfer from ligand to Fe(III) ion.

In the case of aliphatic acids the formation of $[\mathrm{Fe}^{\mathrm{II}}\ldots{}^{\bullet}\mathrm{OOC{-}R}]^{2+}$ radical complex with $\mathrm{COO}^{\bullet}$ - centered radical (mechanism 3a) or carbon-centered $\mathrm{R}^{\bullet}$ radical (mechanism 3b) in coordination sphere of iron ion takes place. From thermodynamical reasons realization of mechanism 3b is more probable as $\mathrm{R{-}COO}^{\bullet}$ radicals are oxidant (redox potential ≥ 2 V)[37,38] and have to reoxidize Fe(II) ion with restoration of initial complex. So one can tentatively proposed that long lifetime and absence of the effective back electron transfer in the radical complexes is due to fast CO_2 detachment and formation of reductive radical $\mathrm{R}^{\bullet}$ in coordination sphere of Fe(II) ion by mechanism 3b.

In the case of SSA the intermolecular electron transfer leads to formation of Fe(II) – phenoxyl radical pair. Phenoxyl radicals with electron-withdrawing groups are rather good oxidants so ultrafast back electron transfer from Fe(II) to coordinated phenoxyl radical with restoration of initial complex is very efficient. Another possible reason of observed photostability of Fe(III) complexes with aromatic ligands is that the delocalization of the "hole" formed upon excitation stabilizes the oxidized ligand with respect to bond splitting and CO_2 loss , enabling thus a effective back electron transfer. Further studies of femtochemistry of aliphatic and aromatic Fe(III) carboxylates combined with quantum-chemistry calculation of properties of possible excited states and radical complexes are needed to clarify photochemistry of these environmentally important species.

Acknowledgements

The work was supported by the RFBR (grants 12-03-00482, 14-03-00692, 14-03-31003) and Novosibirsk State University in framework of joint Laboratory of molecular photonics.

References

1. C. J. Miles, P. L. Brezonik, Environ. Sci. Technol. 1981, **15**, 1089-1095.
2. Y. Zuo, R. D. Jones, *Wat. Res.* 1997, **31**, 850-858.
3. B. F. Voelker, M. M. Morel, B. Sulzberger, *Environ. Sci. Technol.* 1997, **31**, 1004-1011.
4. H. Gao, R. G. Zepp, *Environ. Sci. Technol.* 1998, **32**, 2940-2946.
5. P. Behra, L. Sigg, *Nature* 1990, **344**, 419-421.
6. Y. Zuo, J. Hoigne, *Atmos. Environ.* 1994, **28**, 1231-1239.
7. B. S. Faust, R. G. Zepp, *Environ. Sci. Technol.* 1993, **27**, 2517-2522.
8. Y. Zuo, J. Zhan, *Atmos. Environ.* 2005, **39**, 27-37.
9. Y. Zuo, J. Hoigne, *Science* 1993, **260**, 71-73.
10. W. Feng, D. Nansheng, *Chemosphere* 2000, **41**, 1137-1147.
11. J. W. Hilborn and J. A. Pincock, *J. Am. Chem. Soc.* 1991, **113**, 2683.
12. T. M. Bockman, S. M. Hubig and J. K. Kochi, *J. Org. Chem.* 1997, **62**, 2210-2221.
13. I. P. Pozdnyakov, O. V. Kel, V. F. Plyusnin, V. P. Grivin, N. M. Bazhin, *J. Phys. Chem. A.* 2008, **112**, 8316-8322.
14. X. Zhang, Y. Gong, F. Wu, N. Deng, I. P. Pozdnyakov, E. M. Glebov, V. P. Grivin, V. F. Plyusnin, and N. M. Bazhin, *Russ. Chem. Bull., Int. Ed.* 2009, **58**, 1828-1836.
15. E. M. Glebov, I. P. Pozdnyakov, V. P. Grivin, V. F. Plyusnin, X. Zhang, F. Wu, N. Deng, *Photochem. Photobiol. Sci.* 2011, **10**, 425-430.
16. I. P. Pozdnyakov, F. Wu, A. A. Melnikov, V. P. Grivin, N. M. Bazhin, S. V. Chekalin and V. F. Plyusnin, *Russ. Chem. Bull., Int. Ed.* 2013, **62**, 1579-1585.
17. J. Muller, A. Kikuchi, E. Bill, T. Weyhermuller, P. Hildebrandt, L. Ould-Moussa, K. Wieghardt, *Inorg. Chim. Acta* 2000, **297**, 265-277.
18. V. Nadtochenko, J. Kiwi, *J. Photochem. Photoboil. A:Chem.* 1996, **99**, 145-153.
19. P. Kocot, K. Szaciłowski, Z. Stasicka, *J. Photochem. Photobiol. A: Chem.* 2006, **179**, 176-183.
20. R. Deyrieux, A. Peneloux, *Bull. Soc. Chim. Fr.* 1969, **8**, 2675-2681.
21. J. Chen, H. Zhang, I. V. Tomov, M. Wolfsberg, X. Ding, P. M. Rentzepis, *J. Phys. Chem. A.* 2007, **111**, 9326-9335.
22. S. Goldstein, J. Rabani, *J. Photochem. Photobiol. A: Chem.* 2008, **193**, 50-55.
23. H. B. Abrahamson, A. B. Rezvani, J. G. Brushmiller, *Inorg. Chim. Acta* 1994, **226**, 117-127.
24. G. G. Duka, D. G. Batyr, L. S. Romanchuk and A. Y. Sychev, *Sov. J. Coord. Chem.* 1990, **16**, 93-106.
25. C. Weller, S. Horn, H. Herrmann, *J. Photochem. Photobiol. A: Chem.* 2013, **268**, 24-36.

26. I. P. Pozdnyakov, A. V. Kolomeets, V. F. Plyusnin, A. A. Melnikov, V. O. Kompanets, S. V. Chekalin, N. Tkachenko, H. Lemmetyinen, *Chem. Phys. Lett.* 2012, **530**, 45–48.
27. V. Balzani, V. Carassiti, *Photochemistry of Coordination Compounds,* Acad. Press, London @ New York, 1970, 432 p.
28. A. Vlcek Jr., *Coord. Chem. Rev.* 2000, **200–202**, 933-977.
29. E. A. Juban, J. K. McCusker, *J. Am. Chem. Soc.* 2005, **127**, 6857-6865.
30. J. Chen, H. Zhang, I. V. Tomov, X. Ding, P. M. Rentzepis, *Chem. Phys. Lett.* 2007, **437**, 50–55.
31. I. P. Pozdnyakov, O. V. Kel, V. F. Plyusnin, V. P. Grivin, N. M. Bazhin, *J. Phys. Chem. A.* 2009, **113**, 8820-22.
32. I. P. Pozdnyakov, V. F. Plyusnin, V. P. Grivin, D. Yu. Vorobyev, N. M. Bazhin, S. Pagés and E. Vauthey, *J. Photochem. Photobiol., A: Chem.* 2006, 182, 75-81.
33. I. P. Pozdnyakov, V. F. Plyusnin, N. Tkachenko, H. Lemmetyinen, *Chem. Phys. Lett.* 2007, **445**, 203-207.
34. A. Agren, *Acta Chem. Scand*. 1954, **8**, 266-279.
35. P. J. Reid, C. Silva, P. F. Barbara, L. Karki, J. T. Hupp, *J. Phys. Chem.* 1995, **99**, 2609-2616.
36. K. Tominaga, D. V. Kliner, A. E. Johnson, N. E. Levinger, *J. Chem. Phys.* 1993, **98**, 1228-1243.
37. D. Yu, A. Rauk, D. A. Armstrong, *J. Chem. Soc., Perkin Trans. 2*, 1994, 2207-2215.
38. C. D. Vecitis, T. Lesko, A. J. Colussi, M. R. Hoffmann, *J. Phys. Chem. A.* 2010, **114**, 4968-4980.

Table 1. Observed absorption maxima and lifetimes of the excited states of Fe(III)-carboxylate complexes.[16,21,26]

Complex	λ_{ex} / nm	τ_1 / ps	λ_{max} (τ_1) / nm	τ_2 / ps	λ_{max} (τ_2) / nm
[Fe(Cit)]	400	0.2	< 440	1.4	≈450
	320	N/D*	N/D	≈ 2	≈ 440
$[Fe(Tart)]^+$	400	0.4	< 440	≈ 40	≈ 470
	320	≈ 1	< 440	40	≈ 500
$[Fe(Lact)]^+$	400	0.4	≈465	1.5	≈455
$[Fe(Ox)_3]^{3-}$	400	≈ 1	< 420	N/D	≈430

* - not determined

Table 2. Observed absorption maxima and lifetimes of excited states of Fe(III) complexes with 5-sulfosalicylic acid.[32,33]

Complex	τ_1 / ps	λ_{max} (τ_1) / nm	τ_2 / ps	λ_{max} (τ_2) / nm
FeSSA	0.26	N/D*	1.8	N/D
$Fe(SSA)_2^{3-}$	0.1	600	1.4	< 490
$Fe(SSA)_3^{6-}$	0.17	570	1.5	< 440

* - not determined

FIGURE CAPTURES

Figure 1. Absorption spectra and chemical structures of Fe(III) complexes with citric (1), tartaric (2), and lactic (3) acids.

Figure 2. Femtosecond (λ_{ex} = 400 nm) photolysis of 1.5×10^{-2} M [Fe(Cit)] (*a*) and 1.5×10^{-2} M $[Fe(Tart)]^+$ (*b*) complexes. Kinetic curves of transient absorption change at different wavelengths. Solid lines: best two-exponential fit after reconvolution with the instrument response function.

Figure 3. Femtosecond (λ_{ex} = 320 nm) photolysis of 5×10^{-3} M $[Fe(Tart)]^+$ complex. *a* – transient spectra at different time delay between probe and pump pulses together with inverted absorption spectrum of $[Fe(Tart)]^+$. *b* – kinetic curves of transient absorption change at selected wavelengths. Solid lines: best two-exponential fit.

Figure 4. Femtosecond (λ_{ex} = 400 nm) photolysis of Fe(III) carboxylates. (*a*) –spectrum at zero time for [Fe(Cit)] (*1*), $[Fe(Tart)]^+$ (2) and $[Fe(Lact)]^+$ (3), accordingly; *(b)* –spectrum after the end of ultrafast process for [Fe(Cit)] (*1*), $[Fe(Tart)]^+$ (2) and $[Fe(Lact)]^+$ (3), accordingly. For better comparison data for $[Fe(Lact)]^+$ complex is multiply by factor of 7.

Figure 5. (a) Absorption spectra of Fe(III) complexes with 5-sulfosalicylic acid. (1-3) – FeSSA, $Fe(SSA)_2$, $Fe(SSA)_3$ complexes, correspondingly. (b) Femtosecond (λ_{ex} = 420 nm) photolysis of $Fe(SSA)_3$ complex (3.3×10^{-3} M, pH = 10.3). Kinetic curves of transient absorption change at selected wavelengths. Solid lines: best two-exponential fit after reconvolution with the instrument response function. The apparent shift of “zero” position to the longer times with wavelength increase is due to temporal chirp in the continuum probe pulse.

Figure 6. (a) - Femtosecond (λ_{ex} = 420 nm) photolysis of $Fe(SSA)_3$ complex (3.3×10^{-3} M, pH = 10.3). *1* – spectrum at zero time; *2* – spectrum after the end of ultrafast process. Both spectra are corrected to depopulation of ground state of $Fe(SSA)_3$ (ca. 3×10^{-4} M). Solid curve 3 – the absorption spectrum of ground state of $Fe(SSA)_3$ (3×10^{-4} M). (b) - Generalized potential energy surface diagram for excited-state evolution of $Fe(SSA)_n$ complexes. τ_1 and τ_2 are the time constants of back ET and vibrational cooling, correspondingly.

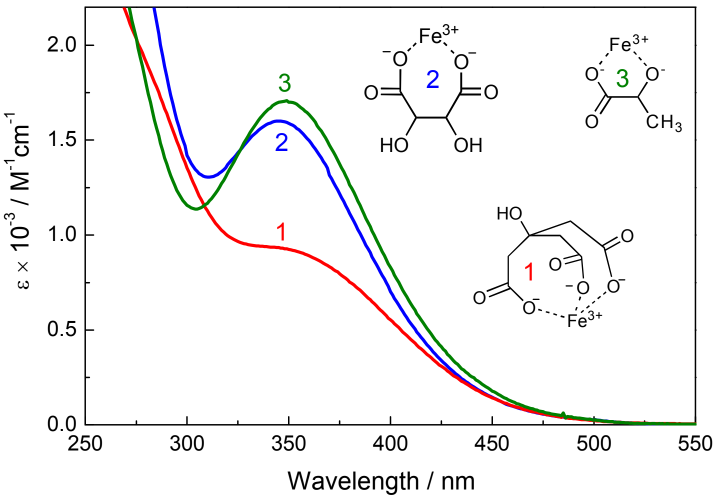

Figure 1

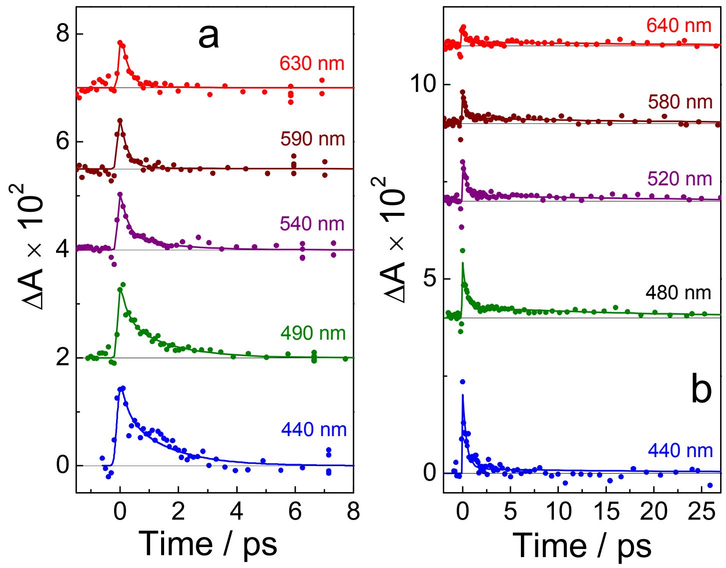

Figure 2

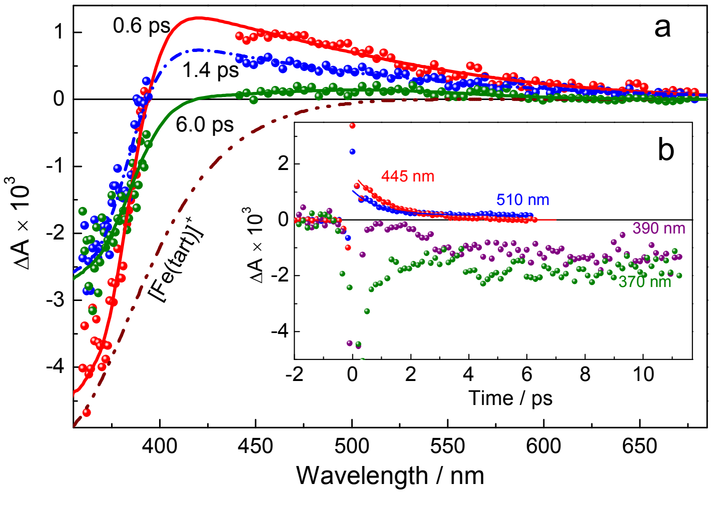

Figure 3

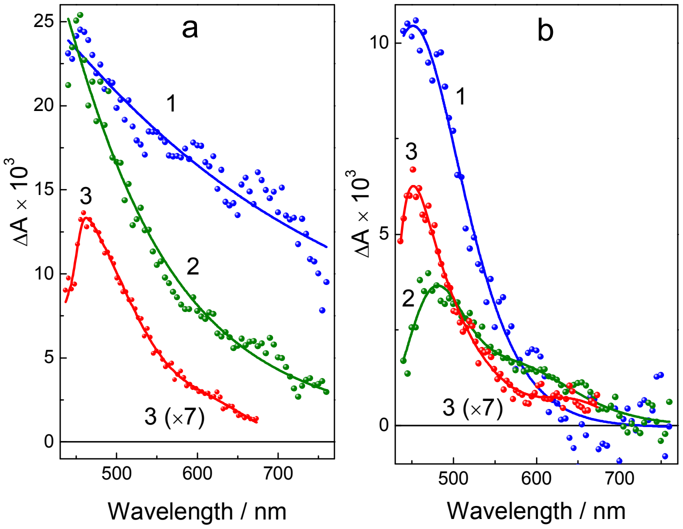

Figure 4

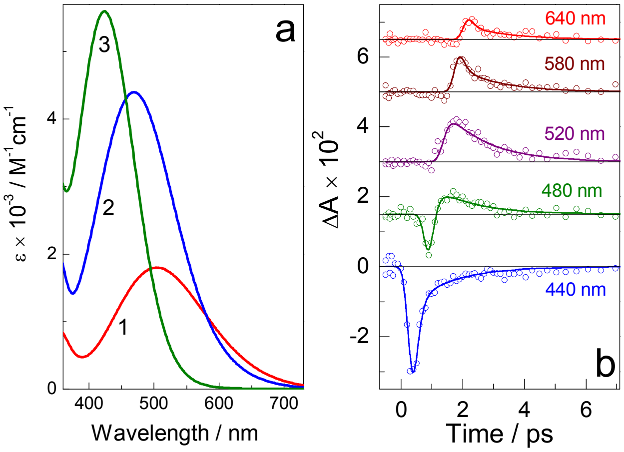

Figure 5

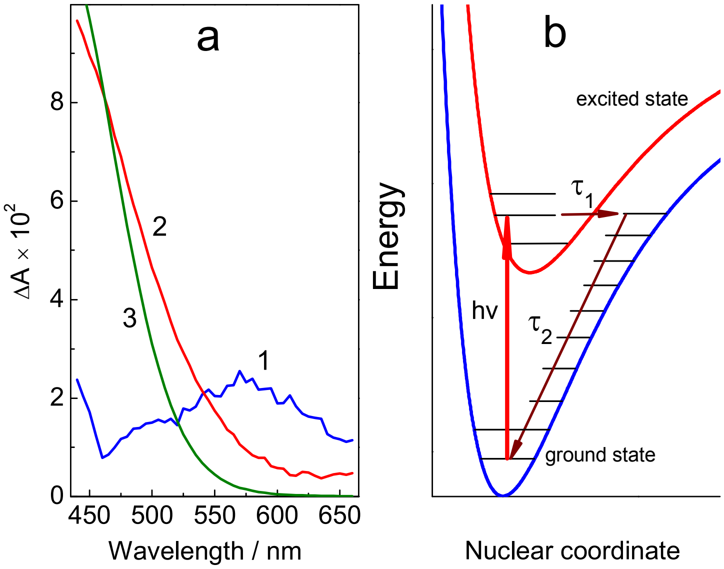

Figure 6

Recent works devoted to investigation of ultrafast processes for several environmentally important Fe(III) carboxylates were observed and discussed.